ANSTO/E-771

Australian Government

Nuclear-based science benefiting all Australians

Possible impact of fixed point sources of SO_2 in NSW to the secondary sulfate measurements at Richmond and the dependence of the background secondary sulphate on meteorological variables

by

J.Crawford

D. D. Cohen

E. Stelcer

Prepared within the Institute for Environmental Research
Australian Nuclear Science and Technology Organisation

May 2010

Abstract

The contribution to secondary sulfate measurements at Richmond, Australia, from known point sources of SO_2 is investigated using air mass back trajectories. The conditional probability function (CPF) shows that contribution for days of high sulfur is from areas north east of the site. This is an area where known point sources of SO_2, such as coal fired power stations, are located. The meteorological conditions associated with high sulfur days are examined and an artificial neural network is employed to determine the relationship between meteorological variables and sulfur measurements after the influence of known point sources was removed. It is shown that temperature and humidity have a nonlinear positive correlation with sulphate measurements, while wind speed, mixing layer depth and rainfall have a negative nonlinear correlation. In addition, the time of day at which air masses reach Richmond from the eastern and western power stations varies, and so thus the altitude at which the power stations are crossed. The time of day, as well as the altitude at which an SO_2 point source was passed, show an impact to the measured sulfate at Richmond, although the extent of this remains to be fully investigated.

Keywords: aerosol, back trajectory, Sydney, secondary sulphate

ISSN 10307745
ISBN 1821268107

Table Of Contents

List of Figures

List of Tables

1 Introduction

SO_2 emissions to the atmosphere undergo oxidation and result in the formation of sulphuric acid (H_2SO_4) and in the presence of ammonia form ammonium sulfate ($(NH4)_2SO_4$). SO_2 has several significant sources which include automobiles, coal fired power stations and industry emissions. Secondary sulfate particles of aerodynamic diameter less than 2.5 micrometers ($PM_{2.5}$) can be any of H_2SO_4, ammonium (bi)sulfate. Foltescu et al., (1996) in their study of gas-to-particle conversion of sulphur and nitrogen point out that the gas-phase oxidation rates exhibit both seasonal and diurnal variations owing to the uneven production of OH. The reactions producing H_2SO_4 and HNO_3 involve sunlight since the SO_2 and NO_2 precursors are oxidised by the OH-radical, produced photo-chemically by the action of solar radiation ($\lambda < 315$ nm) on ozone. The measurements presented here are integrated daily concentrations; thus the diurnal behaviour cannot fully be investigated.

Blumenthal et al. (1984) in their study of pollutants in a grid square of 80x80km, found that concentrations of primary pollutants such as SO_2 and NO_2 were highly variable indicating influence of local sources, whereas secondary pollutants were "reasonably" uniform over 50-150 km. They found that during the night and early morning pollutants were mixed only in the lower few hundred meters above the surface. "Pollutants emitted at the surface during the night were well mixed within the surface layer. Pollutants emitted with an effective plume height greater than few hundred meters usually remained at high concentrations in a poorly mixed layer until the mixing layer deepened due to surface heating during the day. During the early morning, concentrations of SO_2 > 100ppb were frequently seen in elevated layers. Primary pollutants trapped aloft in this manner can react and transport long distances during the night with essentially no deposition. Their presence would not be indicated by surface measurements. Around midday, the atmosphere was generally being well mixed within the lower 1000-1500m msl. However, primary pollutants were usually well-mixed throughout the layer only at relatively large distances from sources, typically > 50km. The median condensation nuclei concentration within the lower 1500m msl during midday was more than twice the median concentration during the night and early morning hours, indicating substantial photochemical formation during daylight." In this study the effect of known point sources of SO_2 to measurements of secondary sulfate are investigated.

Fine particulate matter ($PM_{2.5}$) has been collected at Richmond, NSW and elemental analysis has been carried out using accelerator based ion beam analysis. In this study it is assumed that the sulfur in the samples is secondary sulfate, and the contribution from known SO_2 point sources is investigated using back trajectories. Samples on days for which point sources contributed to the measurement were then removed from the data set. This remaining set of measurements was then used in the training of a neural network to obtain a relationship between meteorological variables and sulfate concentrations. The results of the back trajectory analysis are presented in section 3.2 and those of the neural network analysis are presented in section 3.3.

For the seasonal studies carried out in this work the following breakdown is used; summer (Dec, Jan and Feb), autumn (Mar, Apr and May), winter (Jun, Jul and Aug) and spring (Sep, Oct and Nov).

2 Method

2.1 Study site and local meteorology

Aerosol samples have been collected at Richmond in New South Wales (NSW) Australia from January 2001. Richmond is within the Sydney basin which is bounded by high altitude land to the south, west and north, with Richmond located on the western edge of the basin.

At the site, prevailing wind direction in the summer is onshore winds, also resulting in higher precipitation. The cooler half of the year is associated with low wind speeds and low precipitation conditions from westerly wind during the night and morning period (Chan et al., 2008).

For the Sydney region the estimated SO_2 emission inventory for the year 2007 in tonnes per year was as follows; 261,317 from Coal Power generation, 8,707 from petrol production, 3,433 from aluminium production, 1,712 from industry, 933 from vehicles, 818 from shipping and 3,663 from other sources.

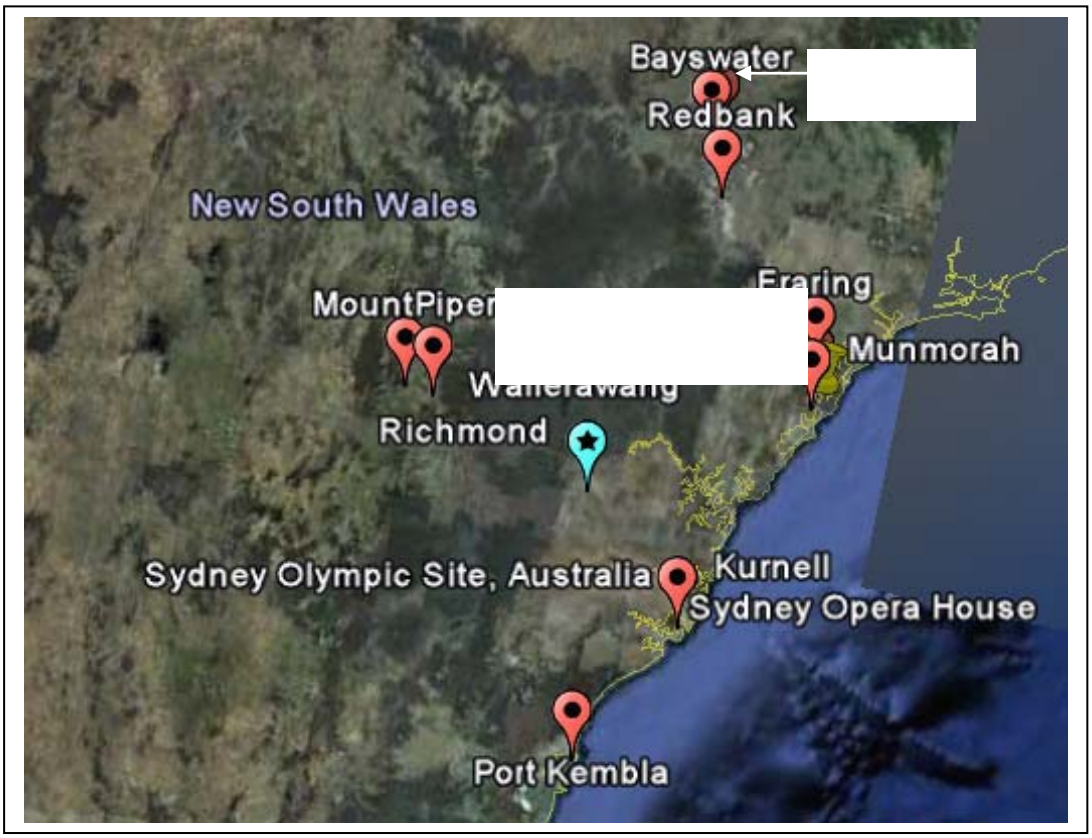

Figure 1: Location of Richmond in blue. SO_2 point sources are shown in orange.

The location of the eight local coal fired power stations is shown in Figure 1, their capacity is shown in Table 1 and their emission of SO_2 for 2007 is presented in Table 2 (NPI 2009). Bayswater is the largest emitter followed by Liddell, Eraring and Mt Piper. An oil refinery plant at Kurnell is also included and so is Port Kembla which is an industrial site south of Sydney where ferrous and non-ferrous metal production is carried out.

Table 1: Location and capacity of 8 power station (DEWHA, 2009), and the location of the Kurnell oil refinery and the Port Kembla industrial site.

Name	Lat (°S)	Long	Distance (km)	Installed Capacity (MW)	Units	MW/Unit	Coal* MT/yr
Bayswater	32.3953	150.9491	137	2640	4	660	5.63
Redbank	32.5784	151.0345	119	150			0.32
Mount Piper	33.3934	149.9705	76	1320	2	660	2.81
Wallerawang	33.404	150.0845	66	1000	2	500	2.13
Liddell	32.3719	150.9783	140	2060	4	515	4.39
Eraring	33.0623	151.5214	94	2640	4	660	5.63
Vales Point B	33.1596	151.5428	90	1320	2	660	2.81
Munmorah	33.2077	151.5393	86	600	2	300	1.28
Kurnell	34	151.2	60				
Port Kembla	34.5	150.9	99				

* Estimated coal consumption by each the power station only, based on the installed capacity and the combined 25 MT/yr of coal usage.

Table 2: Estimated emission inventory of SO_2 from each point source (NPI 2009 for the year 2007).

Point Source	SO2 (kg/year)
Mt Piper	39,000,000
Wallerwang	27,000,000
Bayswater	77,000,000
Liddell	57,000,000
Redbank	2,400,000
Eraring	48,000,000
Vales Point B	14,000,000
Murmorah	7,400,000
Kurnell	3,000,000
Port Kembla	8,800,000

2.2 Aerosol sampling and elemental analysis

The aerosol sampling program constituted 24-hour integrated samples (from midnight to midnight local time) taken twice a week (Wednesday and Sunday) using a cyclone

$PM_{2.5}$ system with 22 l/min flow rate (Cohen et al., 1996). While measurements continue to be made at the sites, for this study measurements up to March 2009 have been used.

Accelerator-based ion beam analysis (IBA) techniques were used to perform the elemental analyses of the aerosol samples (Cohen, 1998; Cohen et al. 2004). These techniques can provide quantitative elemental information on a broad range of elements including: H, Na, Al, Si, P, S, Cl, K, Ca, Ti, V, Cr, Mn, Fe, Co, Ni, Cu, Zn, Br, Pb. In this study is assumed that the measured S is predominantly from secondary sulfate.

2.3 Back Trajectory calculation

The PC version of HYSPLIT v4.0 (HYbrid Single-Particle Lagrangian Integrated Trajectory; Draxler and Rolph, 2003) was used to generate trajectories for each hour of each day on which measurements were made. Two starting heights of 50m and 500m were chosen to be within the atmospheric boundary layer for most sampling days. In comparing HYSPLIT calculated trajectories with tracer gas releases, Draxler (1991) estimated that the model error is between 20% and 30% of the travel distance for this reason we have restricted back trajectories to 7 days along each trajectory for this study.

The trajectories reflect the large-scale atmospheric transport characteristics of the air (Harris and Kahl 1990) and in this study the meteorological data used, (FNL and GDAS files downloaded from the NOAA ftp site; NOAA FNL, NOAA GDAS) has 1° x 1° resolution corresponding to approximately 100 x 100 km grid spacing.

2.4 Point Source Calculations

It has previously been shown through correlation analysis of pollutants from a number of monitoring stations in the Sydney region that for most pollutants, the effect of primary pollutants is only significant within 30km around the site (Duc at al. 2000, study period 1993 and 1994). Thus, in this study, it was assumed that pollutants emitted from the point sources will have the largest impact for 10km around the point source from local meteorology and they can impact downwind arising from synoptic conditions. A program was written which checked which back trajectories passed through a square (with sides of 20km x 20km) centered at each of the point sources. The trajectory as well as other parameters such as the altitude at which it passed over the point source as well as the time it took to get to the measurement site was recorded. Meteorological variables, available in the FNL and GDAS meteorological files (NOAA FNL, NOAA GDAS) such as wind speed, temperature, humidity and sun flux were also recorded and analysed.

2.5 Conditional probability function (CPF)

CPF (Ashbaugh et al., 1985) is used to estimate a conditional probability which indicates the potential of a source region to contribute to high sulfate concentration at the measurement site. Similar to Ashbaugh et al., (1985) the trajectory endpoints are used to determine possible regions contributing to days on which high sulfur concentration were measured. However, sectors are used as opposed to a grided region. The measured daily concentration is assigned to each hour of the day for

which back trajectories were calculated. The CPF is then defined as (notation adapted from Kim and Hopke, 2004):

$$CPF_{\Delta\theta} = \frac{m_{\Delta\theta}}{n_{\Delta\theta}}$$

where $n_{\Delta\theta}$ is the total number of trajectory endpoints falling is sector $\Delta\theta$, and $m_{\Delta\theta}$ is the number of trajectory endpoints falling in sector $\Delta\theta$ for which the measured sulfate exceeded a predefined threshold. In this study, 24 sectors were used ($\Delta\theta$ = 15°) and the data was analysed using two thresholds. One threshold being the mean of the measured sulfur concentration to identify those sectors which were passed by air masses and the measured sulfur at Richmond was larger than the mean, identifying sectors with high probability of recording sulfur concentrations higher than the average (the mean sulfur concentration for this data is 425.69 ng/m^3). The second threshold was the mean plus two standard deviations of the measured suflur concentration (this threshold is 1100.84 ng/m^3). This was used to identify sectors with high probability of contributing to extreme events.

2.6 Artificial Neural Networks (ANNs)

Relationships between meteorological variables and ozone and particulate matter have been investigated using optimisation techniques (Wise and Comrie 2005a, Wise and Comre 2005b). Wise and Comrie (2005b) found that "temperature and mixing height most strongly influence ozone conditions, while moisture levels (particularly relative humidity) are the strongest predictors of particulate matter concentrations in all five cities examined". Authors have argued that linear models "have difficulty capturing the complex relationships between the meteorological variables and ozone" (Thompson et al. 2001) and that modelling fine particulate concentration by regression is more difficult than for ozone.

The advantage of ANNs is that one does not need to determine the form of the function, although there is some control by choosing the number of levels and the activation function. A variety of ANN structures have been proposed and used (Swingler 1996). In this work supervised learning is considered. These ANNs are a form of optimisation, as in linear/nonlinear function fitting, where the function form is normally derived by some knowledge of the system under consideration. In the ANNs approach the function form is not specified, but the size of the ANNs is under user control.

A number of air pollution studies have been based on ANNs (e.g. Kurt et al., 2008, Chelani et al., 2002). Here we examine the influence of temperature, wind speed, mixing layer depth and relative humidity on sulfate measurements with the assistance of a neural network. The available sulfur measurements and the meteorological variables available in the FNL and GDAS files are used to construct a neural network model of sulfur dependence on the meteorological variables, which is later used in an exploratory sense to determine the dependence of sulfur on each meteorological variable in turn, while, keeping all other variables constant.

For the work reported, a public domain package was used (Tveter 1998.

The neural network used has 6 input nodes, one for each meteorological variable, wind speed, temperature, mixing layer depth, rainfall and relative humidity, and one

for the year to allow for possible change in inventory over the years. Five nodes are used in the hidden layer and one node for the output, which is the sulfur concentration.

The data was split into two sets; the training set and the validation set. The network is trained by minimising the error function with respect to the training set. The validation set was used during the training, not to change the weights, but to avoid over training and to check generalisation of the trained network.

3 Results and Discussion

The seasonal average sulfur concentration is presented in Figure 2. There is a clear seasonal trend for sulfur with the lowest concentration in winter and the highest concentration in summer. There is almost similar average concentration in spring and autumn. Because the sulfate is not a primary aerosol but is formed in the atmosphere from the reaction of SO_2 emissions, the atmospheric conditions affect the extent of the secondary sulphate formation. These factors are examined in the following sections.

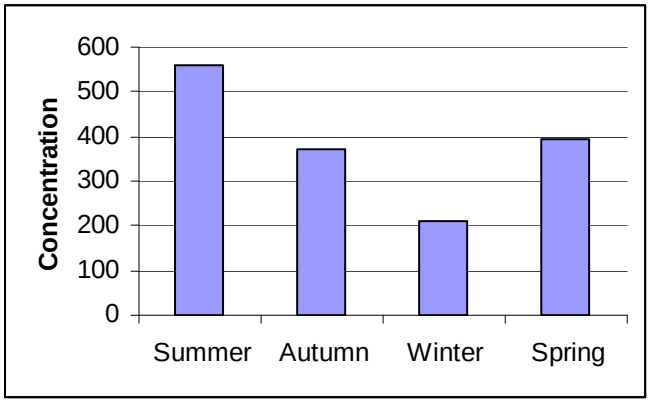

Figure 2: Average seasonal concentration of sulfur at Richmond (ng/m^3).

3.1 Seasonal meteorological conditions

The back trajectory density plots for Richmond are shown in Figure 3a and Figure 3b for winter and summer, respectively. These plots were generated by dividing the region of interest into grid cells of 0.5° by 0.5° resolution. Each value, N, in the grid cell represents the number of trajectories that passed over that grid cell before arriving at Richmond. In summer air masses are predominantly reaching Richmond from eastern region whereas in winter more westerlies are seen. Thus the eastern source regions are passed more frequently in summer, whereas, western areas are passed more frequently in winter. As examined in the following sections the more frequent passage over eastern source regions in summer contributes to the larger summer concentrations (Figure 2).

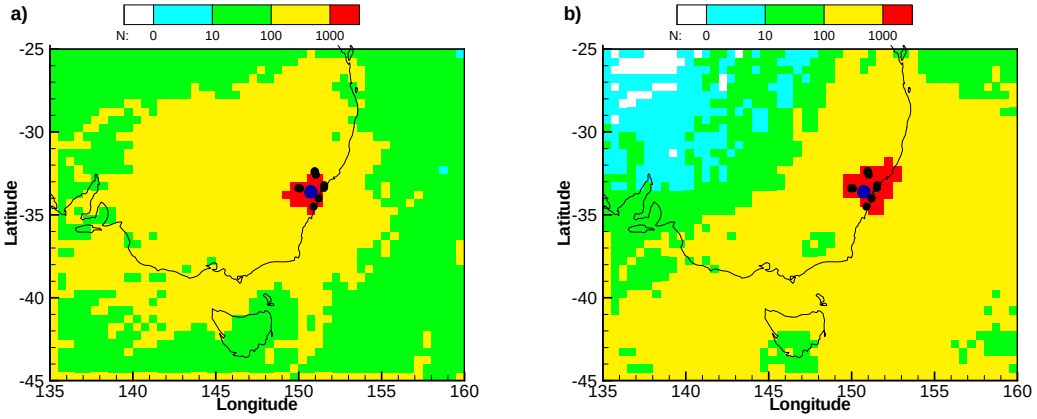

Figure 3: Back trajectory density plot for Richmond for winter days (a) and summer days (b) of aerosol measurements. Richmond is shown as a blue filled circle and the point sources are shown as black filled circles. N is the number of trajectories crossing the grid cell before arriving at Richmond.

3.2 CPF and trajectory passage over point source locations

Table 3 shows the number of trajectories, arriving at Richmond at 50m and 500m altitude, which passed over a point source region, defined by 0.2° by 0.2° square centered at the point source, for winter and summer. In winter Mt Piper is crossed more often than the eastern power stations. For example, for the winter trajectories arriving at Richmond at 50m altitude, Mt Piper is crossed 312 times, whereas Eraring is crossed 111 times. In summer the reverse is true, 496 crossing for Eraring as opposed to 143 for Mt Piper for the 50m back trajectories. The total number of trajectories passing over the identified point sources for all year round and arriving at Richmond at both altitudes (50m and 500m) is also given in the column labeled "All Seasons" in Table 3.

In addition two groups of two columns each are presented in Table 3 (labeled "S > mean" and "S > mean + 2std"). In these columns the number of trajectories passing over the point source for which the measured sulfur concentration at Richmond was greater than the two thresholds are presented. The first threshold used was the mean to identify the number of back trajectories passing over a point source for which the measured concentration at Richmond was greater than the mean of all sulfur measurements. This number is then presented as a percentage of the total trajectories crossing the point source. The results show that Mt Piper, Wallerawong and Port Kembla are less likely to contribute to days of sulfar measurements greater than the mean. The second threshold was specified as the mean of all sulfur measurements plus two times their standard deviation to give extreme events. Once again the same three sources are less likely to contribute to days of measurements greater than the mean plus two standard deviations. In comparison to days when no point source was passed, 10% of the measurements were above the mean and only 0.6% was above the second threshold. The mean sulfur for all days of measurement was 425ng/m^3 and the mean + two standard deviations was 1100ng/m^3.

However, one needs to take care when interpreting these results as the power stations are located in three clusters; the Eraring cluster which consists of Eraring, Munmorah

and Vales Point B, the Bayswater cluster which consists of Bayswater, Liddel and Redbank and the Mt Piper cluster which consists of Mt Piper and Wallerwang. The influence of each power station alone cannot be determined but rather the contribution from each cluster needs to be considered. The distributions of measurements when each cluster only is passed by air masses before arriving at Richmond are considered below.

The CPF, Figure 4, shows that there is a larger probability of recording a concentration greater than the threshold for the passage over the eastern power stations. The CPF is consistent with the results in Table 3, where the eastern power stations show the largest percentage of crossings with sulfur measurements above the two thresholds.

Histograms of sulfur measurements at Richmond for days when at least one point source was passed and days for which no point source was passed are shown in Figures 5a and 5b respectively. When no point sources are passed (referred here to as the background concentration, which is as a result of other SO_2 sources such as vehicle exaust) the peak of the distribution is at 200 (ng/m^3) with an average of 200 (ng/m^3). Whereas when at least one point source is passed for at least one hour on the measurement day, the peak of the distribution is at 300 (ng/m^3) with an average of 482 (ng/m^3). The average for days when a point source was passed is more than double to the background measurements indicating that SO_2 released from point sources has a significant contribution to secondary sulfate measured downwind from the point source.

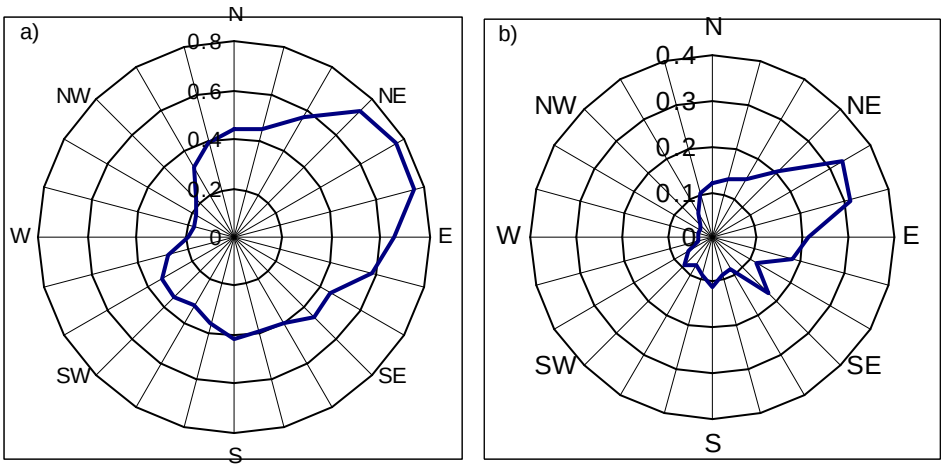

Figure 4: CPF for sulfur at Richmond; with a threshold of the mean (a), and a threshold of the mean plus two standard deviations (b).

Table 3: The number of back trajectories passing in the vicinity of each of the identified point sources, for arrival altitude at Richmond of 50m and 500m. The column marked as % represents the total number of back trajectories that passed over a point source with sulfur concentration > mean of the recorded sulfur plus 2* standard deviation, as a percentage of the total number of trajectories passing over the point source.

	Crossing (50m)		Crossing(500m)		50m+500m	S > mean		S > mean+2std	
Location	Winter	Summer	Winter	Summer	All seasons	Total	%	Total	%
Mt Piper	312	143	263	183	1670	621	37	63	4
Wallerawang	390	149	263	220	1875	711	38	63	3
Bayswater	119	68	75	133	715	486	68	62	9
Liddell	119	67	74	132	710	475	67	54	8
Redbank	137	144	85	132	948	615	65	92	10
Eraring	111	496	84	305	1812	1258	69	153	8
Vales Point B	103	539	88	316	1954	1324	68	158	8
Munmorah	100	540	89	308	1995	1334	67	168	8
Kurnell	155	658	260	532	3364	1617	48	267	8
Port Kembla	268	298	212	144	2176	898	41	82	4

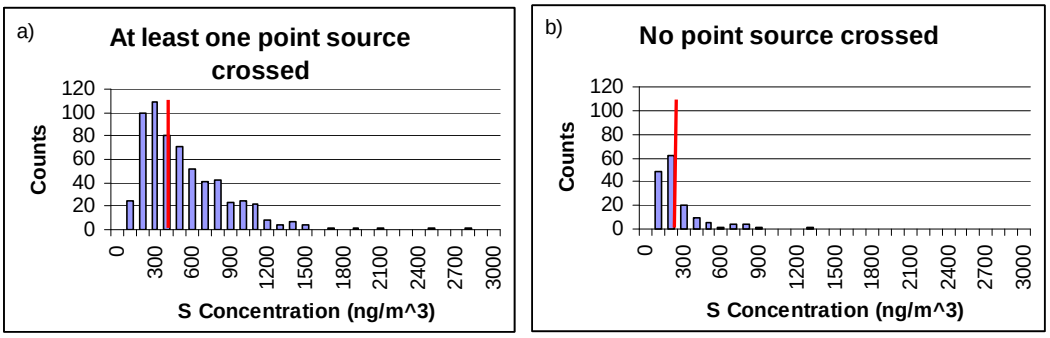

Figure 5: Histograms of sulfur concentration for days when at least one point source is crossed for at least one hour (a) and days when no point source is crossed (b). The average is indicted by the red vertical line.

In order to determine the contribution to sulfate from each power station cluster, the Kurnell oil refinery and the Port Kembla industrial site the measured sulfate on days on which only one of these identified source clusters was crossed were examined. Histograms of sulfur measurements for these days are presented in Figures 6 and 7. The histograms show that the Mt Piper cluster contributes little to the sulfur measured at Richmond (Figure 7), and in fact the average is almost the same as the background, Table 4. On days when Port Kembla only has been crossed the average sulfur measurement is at 265 (ng/m^3), which is slightly above the background. When Kurnell is crossed the average sulfur measurement is at 306 (ng/m^3). The largest concentration is seen from the Eraring and Bayswater clusters, with Eraring having the larger frequency (due to larger number of crossings) of higher than the background average sulfur measurements. Cleary this trend is not only as a result of the emission inventory and distance from the source (Tables 1 and 2), for example Mt Piper located 76 km from Richmond with a release of 39,000,000 kg/year of SO_2 shows little contribution to the measured sulfate, whereas Kurnell located 60km from

Richmond with a release of 3,000,000 kg/year of SO_2 shows a contribution to the measured sulfate. Other factors such as temperature and humidity can affect the conversion of SO_2 to secondary sulfate (Foltescu et al., 1996). The impact of the meteorological variables is analysed in sections 3.3 and the impact of the altitude at which the point source was passed is examined in section 3.5.

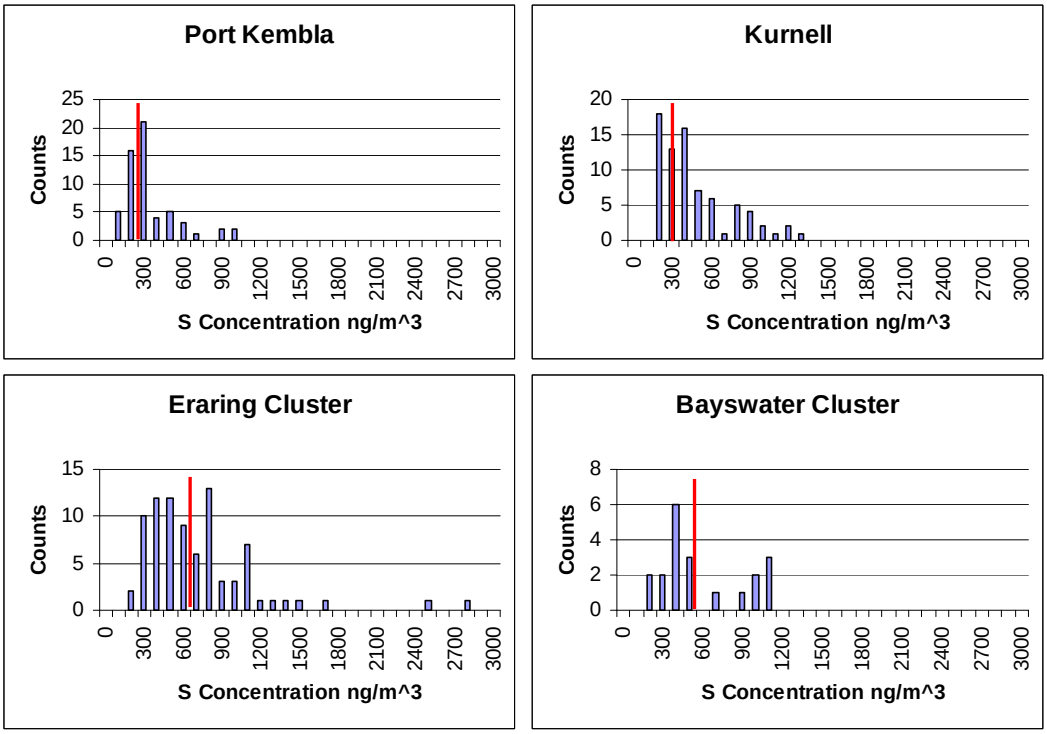

Figure 6: Histogram for sulfur when only a given point source is crossed, counts against concentration in (ng/m^3). Eraring (Eraring, Munmorah, Vales Point B), Bayswater (Bayswater, Liddell, Redbank). The average is shown with the red vertical line.

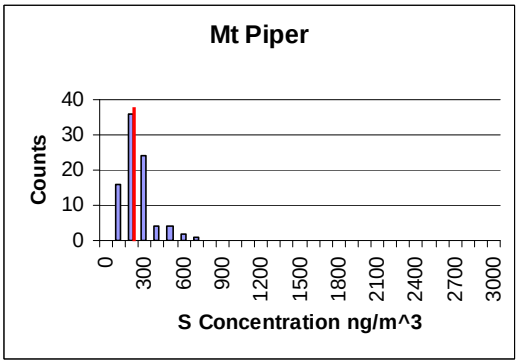

Figure 7: Histogram of sulfur when only Mt Piper and Wallerawang are crossed, counts against concentration in (ng/m^3). The average is shown with a red vertical line.

Table 4: Average sulfur (ng/m^3) for each of the three sets of coal fired power plants, Kurnell and Port Kembla, and when no point source was crossed (background concentration due to sources such as motor vehicles).

Point Source	Average Sulfur
Mt Piper cluster	199
Bayswater cluster	534
Eraring cluster	665
Kurnell	306
Port Kembla	265
No point Source	200

3.3 Correlation with meteorological variables when no point source has been crossed

The concentrations measured at a site are a function of a number of factors, such as the release and transport and mixing, deposition and the depth of the mixing layer. In addition for the formation of secondary sulfate other factors become important, such as humidity, temperature, sunlight hours etc. In this section the correlation of sulfur concentrations, for days on which no point source was passed, with a number of meteorological variables is undertaken. The variables chosen here are those that are available in the meteorological files; mixing layer depth, rainfall, temperature, wind speed and humidity. The values of each of these variables are extracted from the NOAA FNL and GDAS files at the measurement site (Richmond), with rainfall being the total for the last 6 hours along the trajectory path.

A number of studies have undertaken a linear regression of selected meteorological variables with measured aerosol concentrations. Scatter plots of sulfur concentration against the selected variables is shown in Figure 8. There is a negative correlation with mixing layer depth, rainfall and wind speed. The correlation with temperature and humidity is positive. However, from the scatter plots it becomes apparent that the correlation is not simply a linear one, hence an ANN was chosen to analyse these dependencies.

For the ANN study a total of 157 observations were available, from which 15 (~10%) were selected as the validation set (every 10th observation was selected). For the training each variable was normalised by dividing by its maximum, so that values between 0 and 1 only were used for the training. The divisors were as follows; year 10, wind speed 40, temperature 30, mixing layer depth 1500, rainfall 10, relative humidity 100 and sulfur 1500. The ANN had 6 input nodes; one for each of the year (to account for a change in emission rates for each year), wind speed, temperature, mixing layer depth, rainfall and humidity. The assumption for the release rate was that it was constant for a given year.

The goodness of the obtained fit can be determined for Figure 9, which shows the predicted sulfur values when using the neural network against the measured values of sulfur. The line of best fit has a slope of 0.95 and r^2 of 0.83. This is a reasonable fit given that the values used for the meteorological variables were not local observations, but were generated from 1° by 1° resolution meteorological data files

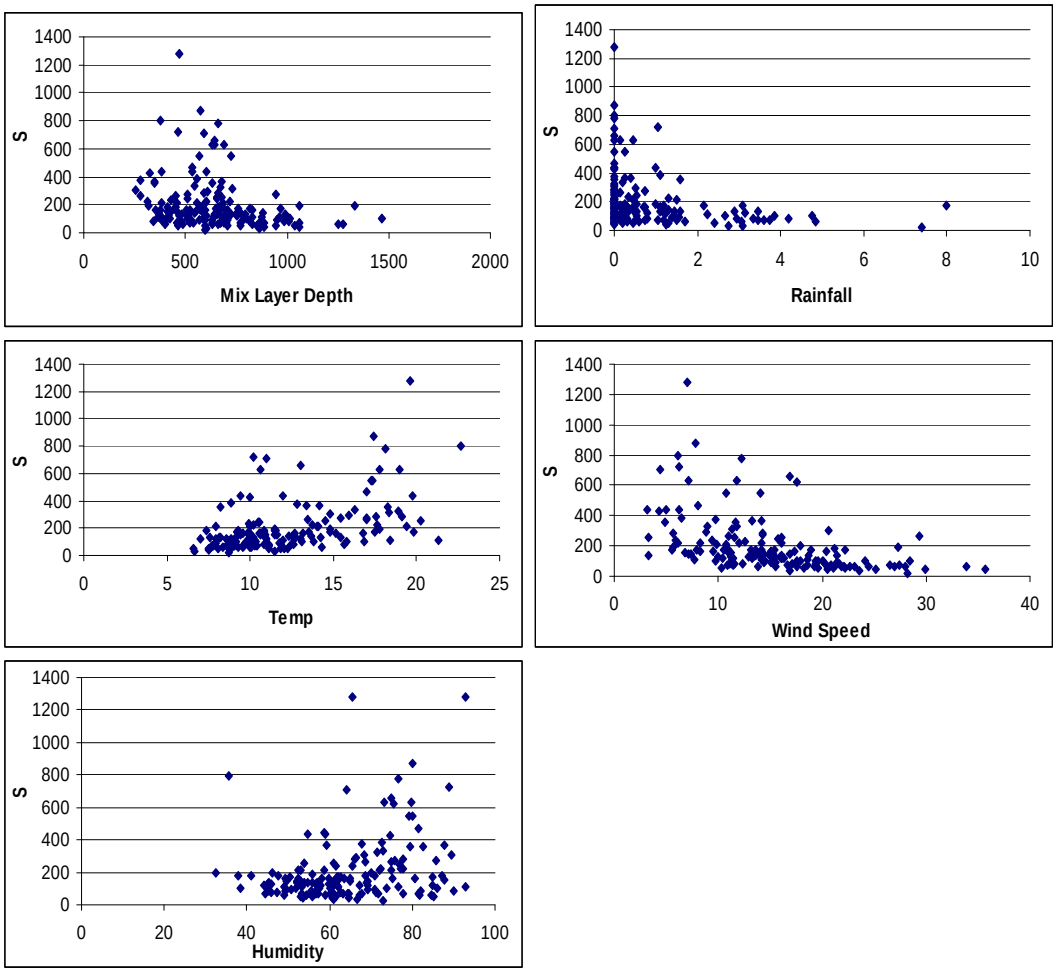

Figure 8: Scatter plots of sulfur (S) concentration (ng/m^3) against selected meteorological variables; mixing layer depth (m), rainfall (total in mm for the last 6 hours), temperature (°C), wind speed (km/hour), humidity (%) when no point source has been crossed.

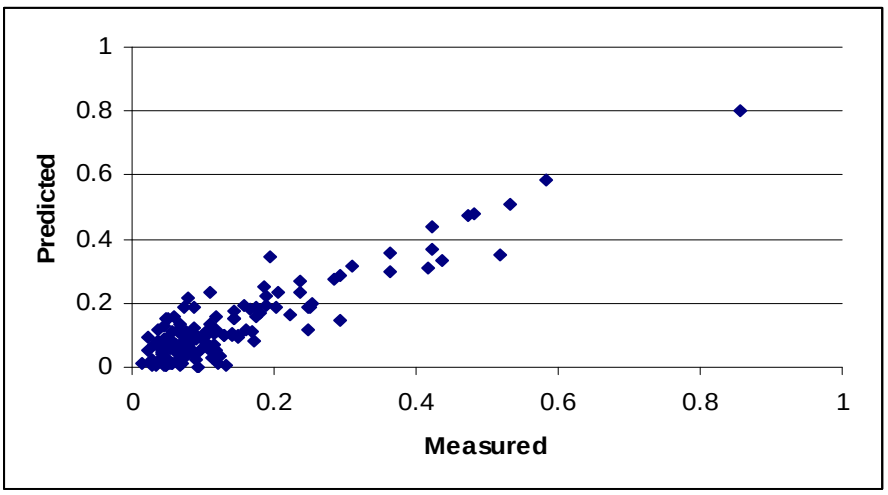

Figure 9: Scatter plot of normalised sulfur (S) as predicted by the neural network against normalised measured sulfur. The normalisation was achieved by dividing each concentration by the maximum.

Once the training was completed a value of 0.3 for the year, 0.2 for wind speed, 0.8 for temperature, 0.5 for mixing layer depth, 0.1 for rainfall and 0.9 for humidity were chosen as the base case. These values were chosen on the basis that they presented favourable conditions for sulfate formation. The neural network was then used to make predictions for the range of each variable (i.e. 0.1 to 0.9 and 0.1 increments), in turn, while keeping all other variables to their base case value. The results are presented in Figure 10. We can see that there is a nonlinear increase in sulfur corresponding to increase in temperature and humidity and a nonlinear decrease with increasing wind speed, rainfall and mixing layer depth. There is a low value of sulfur when the mixing layer depth takes on the normalised value of 0.1. This is not surprising as there was no data for normalised mixing layer depth values less that 0.17, corresponding to a mixing layer depth of 255m.

There is a slight increase of predicted sulfur as we go from normalised year 0.1 (year 1) to year 0.4 (year 4) and then a decrease. This trend is observed in the measured sulfur concentration, Figure 11.

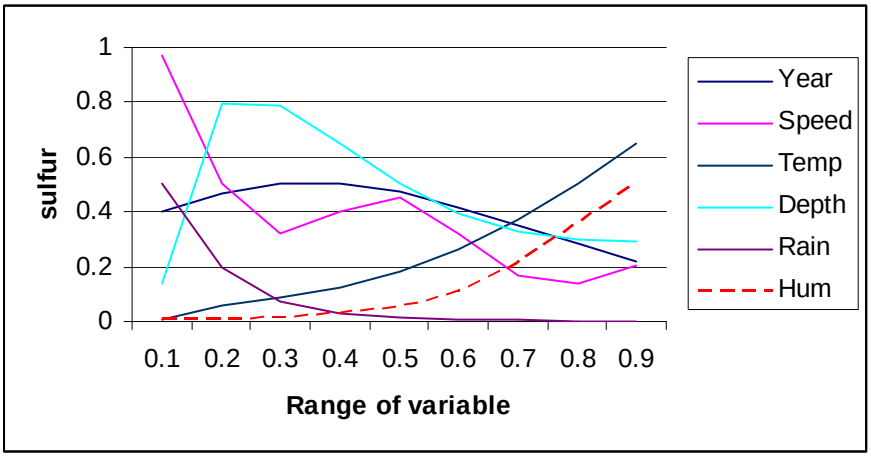

Figure 10: Normalised sulfur vales predicted by the neural network for each meteorological variable over its normalised range while all other variables are set at their base case value.

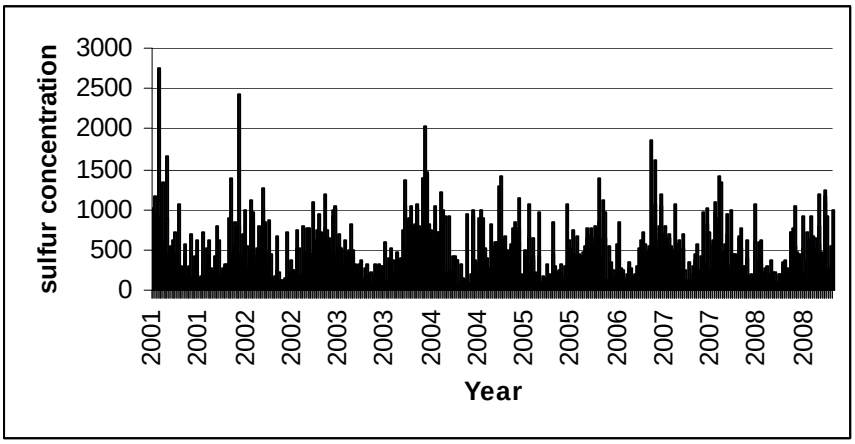

Figure 11: Measured sulfur concentration (ng/m^3) against the year of measurement.

3.4 Correlation with meteorological variables when a point source has been crossed.

The average and standard deviations of the meteorological variables for days when Mt Piper and Eraring were passed by back trajectories before arriving at Richmond are shown in Table 5. Using the results from section 3.3, we see that the meteorological conditions are more suitable for secondary sulfate formation on days that Eraring is passed, e.g. wind speed is lower and humidity is higher. A similar correlation between sulfur and mixing layer depth, rainfall, temperature and wind speed is seen on days when no point source was crossed (Figure 8) and on days when a point source is crossed (Figure 12). Increasing humidity still shows an increase in sulfur, however the increase is not as large as for the days when no point source was crossed.

Table 5: Average and standard deviation of meteorological variables of days on which the back trajectories passed over Mt Piper and Eraring, for trajectories arriving at 50m.

	Mt Piper		Eraring	
	Mean	Std	Mean	Std
Temperature (°C)	13	5	18	4
Wind Speed (km/hr)	21	9.6	13.6	4.3
Altitude (m)	225	263	22.9	25
Rainfall (mm in last 6 hr)	0.99	2	0.42	1.4
Humidity (%)	54	14	69	10.9
Hours	8.79	5	10.64	5.6
Sun Flux (watts)	199	191	268	181
Mixing Layer Depth (m)	679	473	523	216
S (ng/m^3)	198	119	665	435

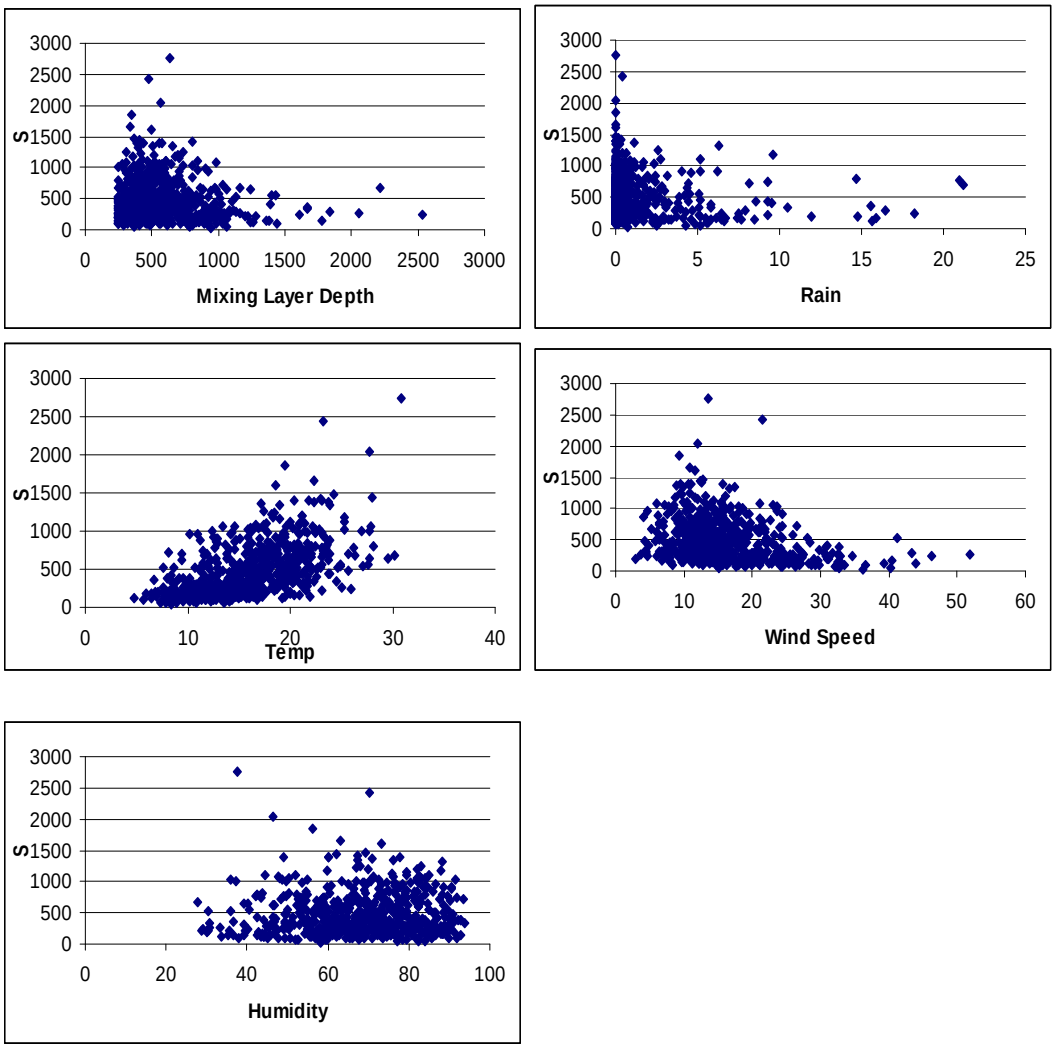

Figure 12: Scatter plots of sulfur (S) concentration (ng/m^3) against selected meteorological variables; mixing layer depth (m), rainfall (total in mm for the last 6 hours), temperature (°C), wind speed (km/hour), humidity (%) for days on which at least one of the point sources has been crossed.

3.5 Impact of air mass altitude at the point source

When a point source is crossed there is the additional factor that is of importance, i.e. the altitude at which the air mass passed over the point source and how this compares with the effective release height. From Table 5, trajectories arriving at Richmond at 50m, on average cross over Mt Piper at 225m altitude. Back trajectories arriving at Richmond at 50m cross Eraring on average at 23m altitude. On average Bayswater is crossed at 247m altitude for trajectories arriving at Richmond at 50m. Trajectories arriving at Richmond at 500m cross Mt Piper, Eraring and Bayswater at 824m, 472m and 739m respectively. The scatter plots in Figure 13 show that there is a positive correlation between the altitudes at which Eraring was passed by the air mass, at least for altitude below 100m, however there is insufficient data to assess the impact of higher altitudes. The time for the air mass to reach Richmond has no clear correlation with sulfur and neither has the sun flux. For air masses arriving at Richmond at 500m altitude, for Eraring, there is no correlation between the altitude at which they crossed Eraring and the sulfar measured at Richmond.

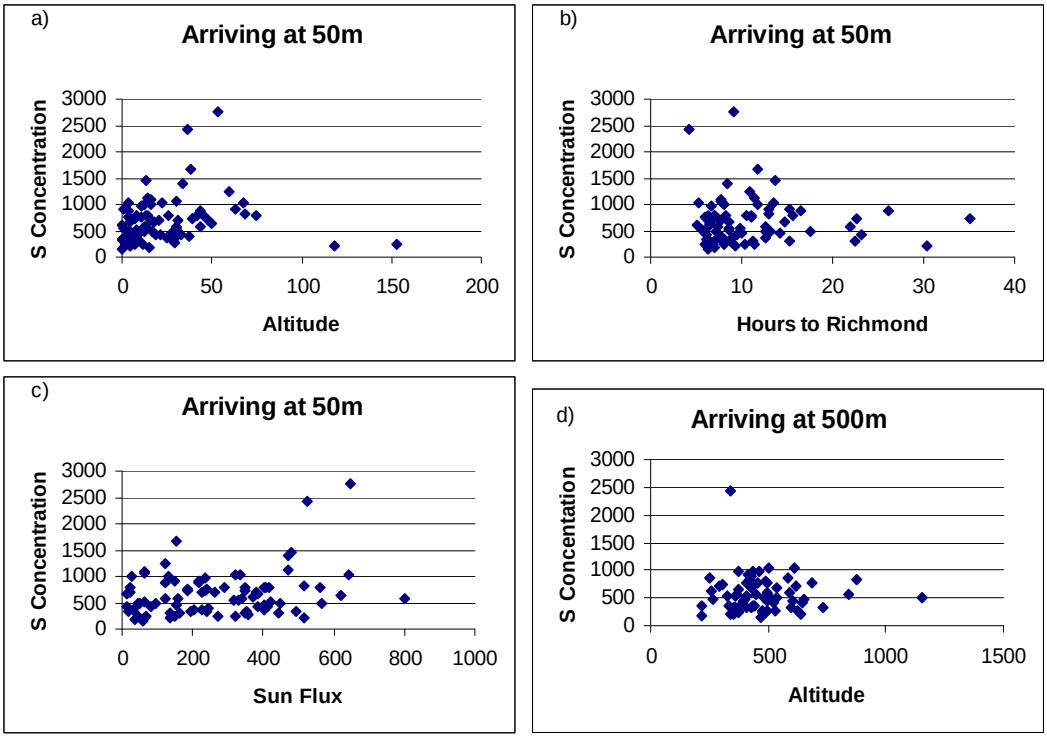

Figure 13: Scatter plots of sulfur (S, ng/m^3) with altitude (m) at which Eraring cluster was passed by the air mass arriving at Richmond at 50m (a) and those arriving at 500m (d), time it took to travel from Eraring to Richmond and the sun flux (watts) at Richmond.

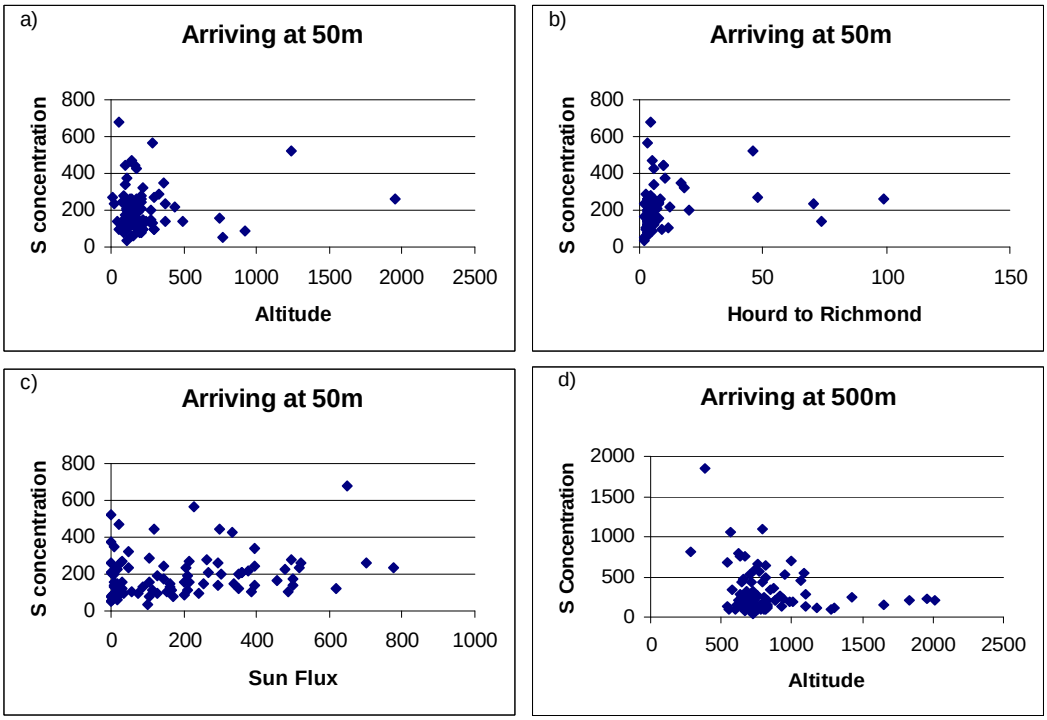

Figure 14: Scatter plots of sulfur (S, ng/m^3) with altitude (m) at which Mt Piper cluster was passed by air masses for the 50m arrival height (a) and for the 500m (d), time it took to travel from Mt Piper to Richmond (b) and the sun flux (watts) at Richmond (c).

The scatter plots in Figure 14 show that there is a positive correlation between the altitude at which the air mass passed over Mt Piper and the measured sulfur at Richmond, which levels of at an altitude of about 500m. For trajectories arriving at 500m at Richmond there is a reduction in the sulfur concentration for at altitude of about 1200m at which the air mass passed over Mt Piper. Similarly there some correlation with the length of time it takes for the air mass to reach Richmond, with higher concentrations for about 20 hours. However, one needs to be careful with the interpretation of these results for Mt Piper as the concentration of sulfur measured at Richmond is the same as the background (i.e. that contributed from other sources, e.g. vehicles)

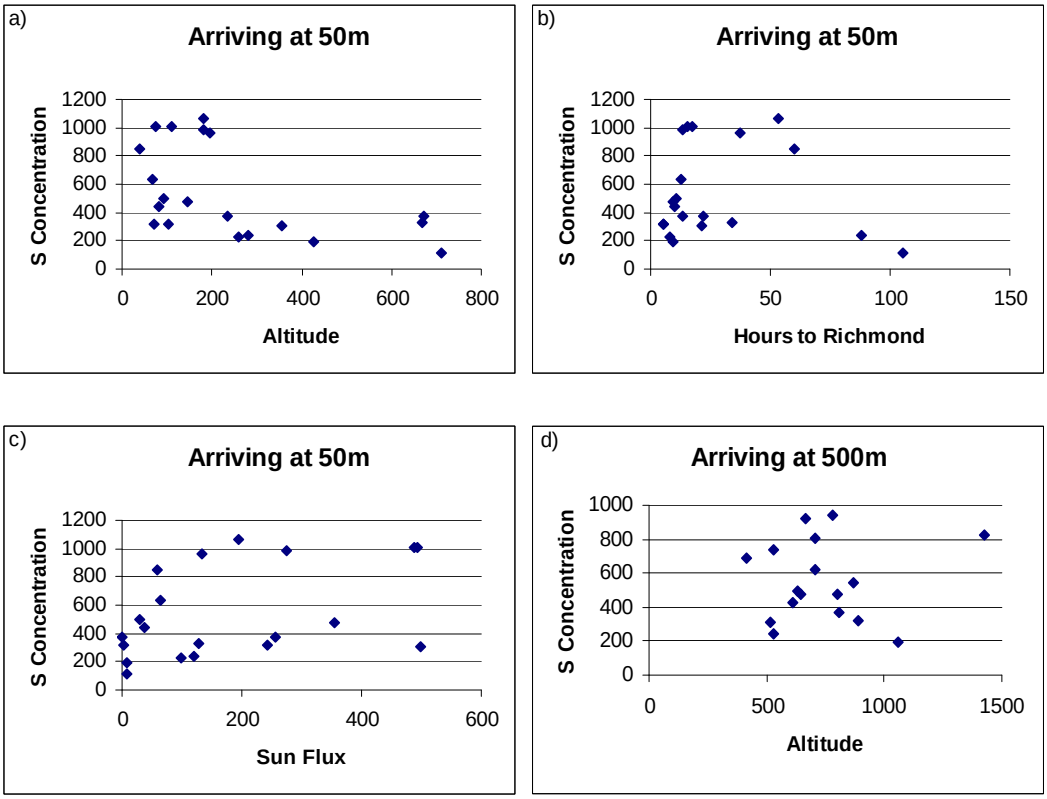

Figure 15: Scatter plots of sulfur (S, ng/m^3) with altitude (m) at which Bayswater cluster was passed, for 50m arriving altitude (a) and for 500m arriving altitude (d), time it took to travel from Bayswater to Richmond (b) and the sun flux (watts) at Richmond (c).

The scatter plots in Figure 15 show that there is a positive correlation between the altitude at which the air mass passed over the Bayswater cluster and the measured sulfur at Richmond, which levels of at an altitude of about 200m for those air masses arriving at an altitude of 50m at Richmond. For air masses arriving at 500m at Richmond there is no correlation between the measured sulfur and the altitude at which the air mass crossed Bayswater. Similarly there some correlation with the length of time it takes for the air mass to reach Richmond, with higher concentrations for about 70 hours.

From these plots we can conclude that the altitude at which the air mass has passed over the point source has an impact on the measurements at the receptor site. However, there is insufficient data at the higher altitudes to draw a conclusion as what

the maximum altitude at which SO_2 will be entrained by an air parcel. This is an area that needs further investigation.

3.6 Impact of time of day

The time of day of air mass passage needs to be examined as there is a diurnal variation of sulfate formation due to sunlight. Figure 16, shows that in winter (Figure 16 a) trajectories from Mt Piper are more likely to arrive at Richmond in the late afternoon, whereas in summer (Figure 16 b) they are more likely to arrive in the morning (a period off less favourable conditions for sulfate formation). For Eraring in summer, when high sulfur is recorded, the trajectories arrive during the day and evening, thus encountering more favourable conditions of SO_2 to sulfate conversion.

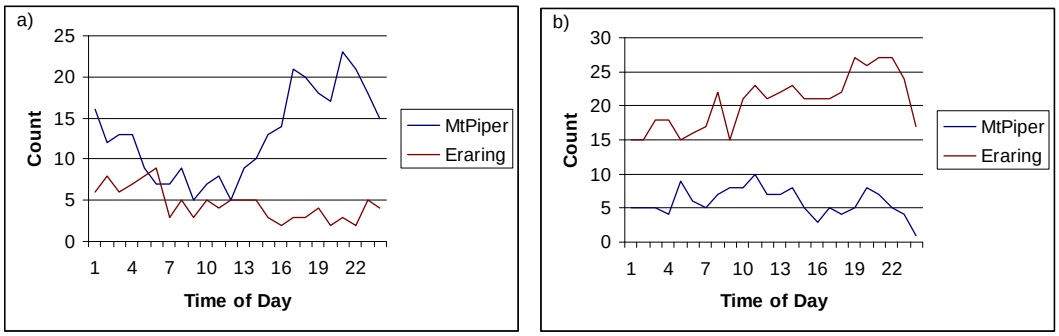

Figure 16: Time of day at which trajectories arrive at Richmond from Mt Piper and Eraring, for winter (a) and summer (b).

4 Conclusion

Using back trajectories to separate days of measurements based on air mass passage over known point source locations of SO_2 has enabled the analysis of contribution to the sulfur measurements at Richmond form the identified point sources. From the sulfur concentration distributions it is seen that Bayswater and Eraring have an impact on the measured sulfur at Richmond.

Further, by removing the influence from point sources an ANN was able to be trained to obtain a relationship between the meteorological variables and sulfur measurements for the background concentration of SO_2, being from such sources as vehicles. It was found that a nonlinear relationship exists with the considered variables.

5 Acknowledgments

The NOAA Air Resources Laboratory (ARL) made available the HYSPLIT transport and dispersion model and the relevant input files for generation of back trajectories used in this paper.

6 References

Ashbaugh L.L, Malm W.C., Sadeh W.Z. 1985. A residence time probability analysis of sulfur concentrations at Grand Canyon National Park. Atmospheric Environment 19(8) 1263-1270.

Bishop C.M. 1997. Neural Networks for Pattern Recognition, Clarendon Press, Oxford, ISBN 0-19-853864-2.

Blumenthal, D.L, McDonald J.A., 1984. Three-dimensional pollutant distribution and mixing layer structure in the northeast U.S., Summary of Sulfate Regional Experiment (SURE) aircraft measurements. Atmospheric Environment 18 (4) 733-749.

Chan Y-C., Cohen D.D., Hawas O., Stelcer E., Simpson R., Denison L., Wong N., Hodge M., Comino E. and Stewart Carswell, 2008: Apportionment of sources of fine and coarse particles in four major Australian cities by positive matrix factorisation. Atmospheric Environment 42, 374-389.

Chelani A.B., Chalapati Rao C.V, Phadke K.M., Hasan M.Z. 2002. Prediction of sulphur dioxide concentration using artificial neural networks. Environmental Modelling and Software 17, 161-168.

Cohen D.D., Bailey G.M. and Kondepudi R., 1996: Elemental analysis by PIXE and other IBA techniques and their application to source fingerprinting of atmospheric fine particle pollution, Nucl. Instr. and Methods 109, 218-226.

Cohen D.D., 1998: Characterisation of atmospheric fine particles using IBA techniques. Nuclear Instruments and Methods in Physics Research B136-B138, 14-22.

Cohen D.D, Garton D., Stelcer E., Hawes O., 2004: Accelerator based studies of atmospheric pollution processes. Radiation Physics and Chemistry 71, 758-567.

DEWHA, 2009:Australian Government, Depaetment of the Environment, Water, Heritage and the Arts, http://www.ga.gov.au/fossil_fuel/, accessed March 2009.

Draxler, R.R. 1991: The accuracy of trajectories during ANATEX calculated using dynamic model analysis versus rawinsonde observations. Journal of Applied Meteorology 30, 1466-1467.

Draxler R.R and Rolph G.D., 2003: Hybrid Single-Particle Lagrangian Integrated Trajectory (HYSPLIT), model. http://www.arl.noaa.gov/ready/hysplit4.html.

Duc H., Shannon I., Azzi M. 2000: Spatial distribution characteristics of some air pollutants in Sydeny. Mathematics and Computers in Simulation 54 1-21.

Foltescu V.L., Selin E., Isakson J. and Oblad M. 1996: Gas-to-particle conversion of sulphur and nitrogen compounds as studied at marine stations in northern Europe, Atmospheric Environment Vol 30 No 18 pp 3129-3140.

Harris J.M. and Kahl J., 1990: A descriptive Atmospheric Transport Climatology for the Manua Loa Observatory, Using Clustered Trajectories. Journal of Geophysical Research 95 (D9) 13,651-13,667.

Kim E., Hopke P.K., 2004. Comparison between Conditional Probability Function and Nonparametric Regression for Fine Particle Source Direction. Atmospheric Environment 38, 4667-4673.

Kurt A., Gulbagci B., Karaca F., Alagha O., 2008, A online air pollution forecasting system using neural networks. Environment International 34, 592-598.

NOAA FNL: ftp://gus.arlhq.noaa.gov/pub/new-archives/fnl/
NOAA GDAS: ftp://gus.arlhq.noaa.gov/pub/archives/gdas1/

NPI 2009: National pollutant inventory. http://www.npi.gov.au/cgi-bin/npidbsearch.pl?proc=facility, accessed May 2009.

Swingler K., 1996. Applying Neural Networks: A practical Guide. Academic Press, London, ISBN 0-12-679170-8.

Thompson M.L., Reynolds J., Cox L.H., Guttorp P., Sampson P.D., 2001. A review of statistical methods for meteorological adjustment of tropospheric ozone. Atmospheric Environment 35 617-630.

Tveter D.R. 1998Student Version Basis of AI Backprop http://www.boutell.com/lsm/lsmbyid.cgi/001604

Wise E.K., Comrie A.C., 2005a. Extending the Kolmogorov-Zurbenko Filter: Application to Ozone, Particulate Matter, and Meteorological Trens. Air and Waste Management Association, 55(8), 1208-1216

Wise E.K., Comrie A.C., 2005b. Meteorologically adjusted urban air quality trends in the Southwestern United States. Atmospheric Environment, 39 2969-2980.